Semiempirical Calculations of the Electronic Absorption Spectra of Vitamin B_6 Derivatives in the Active Site of Mitochondrial Aspartate Aminotransferase

P. A. Clark, J. N. Jansonius, and E. L. Mehler*

Contribution from the Department of Structural Biology, Biocenter of the University of Basel, Klingelbergstrasse 70, CH-4056 Basel, Switzerland. *Received August 3, 1992*

Abstract: The electronic absorption spectra of derivatives of the vitamin B_6-related cofactor of mitochondrial aspartate aminotransferase (mAspAT) have been calculated using a semiempirical, all-valence-electron INDO/S method with configuration interaction. Several models of partial active site structures were studied to assess the effects of the protein environment on the spectra of the coenzyme. The models include either of two forms of the cofactor, i.e., the pyridoxal 5'-phosphate (PLP) internal aldimine or the noncovalently bound pyridoxamine 5'-phosphate (PMP), and groups which model residues interacting directly or indirectly with PLP or PMP. Residues which are hydrogen bonded to the ring moiety of the cofactor include Asn194, Asp222, and Tyr225. In addition, the indole of Trp140 could be involved in π-stacking interactions with the pyridine ring. His143, Ser139, and a water molecule modulate the effect of Asp222 by forming an H-bonded network with this residue. The effects of these residues on the spectra of PLP and PMP were analyzed by calculations on models consisting of the cofactor and various combinations of the above residues. Geometries were taken from X-ray structural data, and hydrogen atom positions were optimized using the AM1 Hamiltonian. Results for both the protonated and unprotonated PLP aldimines are in good agreement with measured solution spectra. The calculations predict that the effect of the active site residues included in the model generally lead to a blue shift of the spectrum of the isolated cofactor. A further important result of these calculations is that, for a proper description of the effect of the charged Asp222 on the chromophore's spectrum, residues interacting with the former must also be included in the calculation. This appears to be primarily due to the delocalization of the charge due to the H-bonded network which links the charged species to the cofactor and other residues. The spectra for the PMP form show a similar response to the inclusion of active site residues as those for the PLP aldimine, although the quantitative agreement with experiment is not as satisfactory. The orientations of the calculated transition dipole moment vectors of the chromophore agree to within experimental error with the observed values. Effects of different protonation states and cofactor conformations on the spectra are also discussed.

Introduction

Pyridoxal 5'-phosphate (PLP) is a vitamin B_6 derivative which functions as the cofactor in a large family of enzymes that catalyze manifold reactions in amino acid metabolism. These reactions pass through a series of covalent intermediates that can often be distinguished by their characteristic absorption spectra in the 300–500-nm region. Aspartate:2-oxoglutarate aminotransferase (AspAT; EC 2.6.1.1) is probably the most thoroughly investigated representative of this enzyme family. It catalyzes the reversible reaction

L-aspartate + 2-oxoglutarate ↔ oxaloacetate + L-glutamate

in which the amino acid substrate in the forward half-reaction is transformed into the corresponding oxo acid product, the amino group being temporarily stored on the cofactor in its pyridoxamine 5'-phosphate (PMP) form. In the reverse half-reaction, an oxo acid substrate takes up the amino group and leaves the enzyme as the L-amino acid, while the cofactor is restored to its original PLP form. The chemical structures of the intermediates in the transamination reaction and their electronic absorption spectra have been identified by comparison with extensive data on the free cofactor and its derivatives as well as related structures.[1,2] Higher animals possess distinct cytosolic and mitochondrial AspAT's with typically 45–50% amino acid sequence identity[3,4] and quite similar absorption spectra.[5] Scheme I displays some of the enzyme forms and catalytic intermediates with their characteristic absorption maxima. The cofactor PLP forms a Schiff base, or aldimine, with Lys258 which at high pH (I) absorbs at about 360 nm; protonation of the aldimine N at low pH (II) shifts this band to about 430 nm. The external aldimine formed by the PLP–

Scheme I

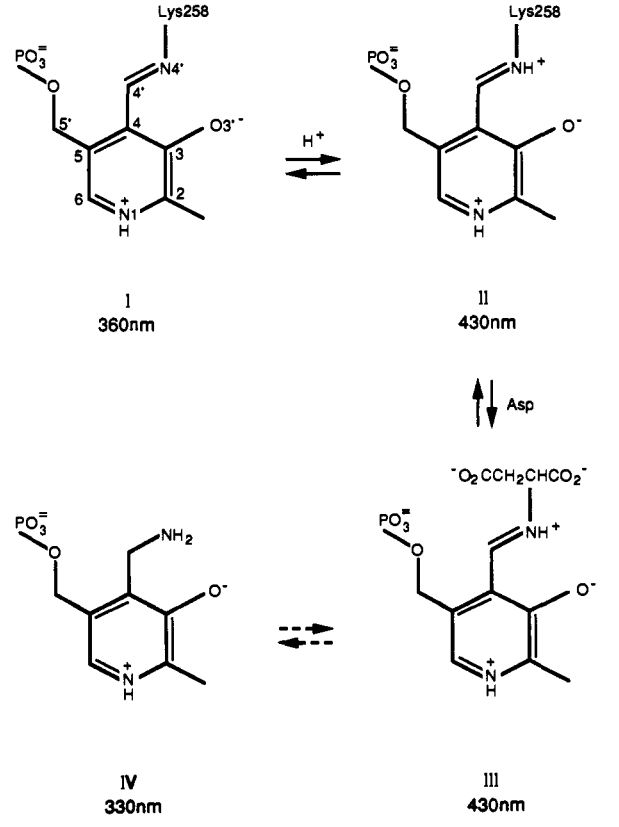

(1) Braunstein, A. E. In *The Enzymes*; Boyer, P. D., Ed.; Academic Press: New York, 1973; Vol. 9, pp 379–481.
(2) Christen, P.; Metzler, D. E., Eds. *Transaminases*; John Wiley: New York, 1985.
(3) Christen, P.; Graf-Hausner, U.; Bossa, F.; Doonan, S. In *Transaminases* (Christen, P., Metzler, D. E., Eds.); John Wiley: New York, 1985; pp 173–185.
(4) Doonan, S.; Martini, F.; Angelaccio, S.; Pascarella, S.; Barra, D.; Bossa, F. *J. Mol. Evol.* **1986**, *23*, 328–335.
(5) Michuda, C. M.; Martinez-Carrion, M. *J. Biol. Chem.* **1969**, *244*, 5920–5927.

0002-7863/93/1515-1894$04.00/0

Scheme II

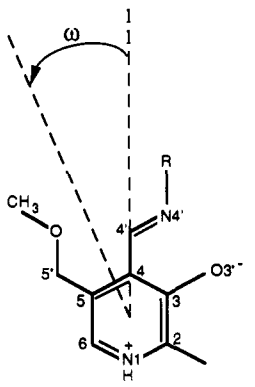

Scheme III

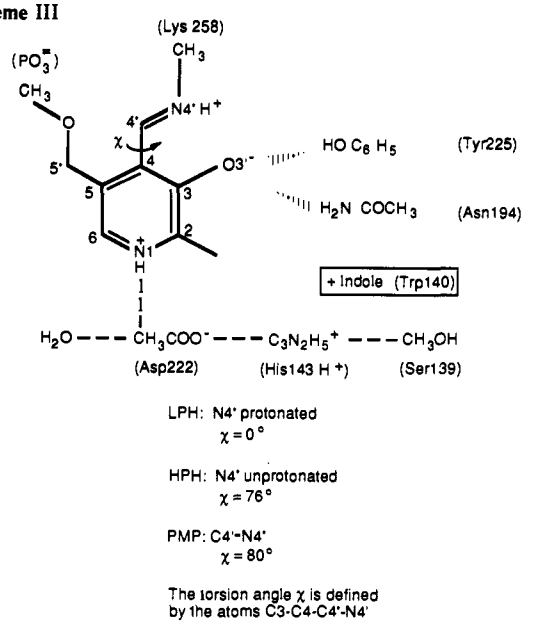

enzyme with the substrate (III) also absorbs at about 430 nm, whereas the pyridoxamine phosphate (PMP) form of the cofactor present at the end of the half-reaction (IV) absorbs at about 330 nm.

The transition dipole moment (TDM) of each absorption band lies in the plane of the cofactor's pyridine ring, but its direction, which is measured by the angle ω (see Scheme II), is wavelength-dependent and thus varies among cofactor-substrate catalytic intermediates along the reaction pathway.[6] If these TDM directions were known, linear dichroism experiments on, for example, orthorhombic crystals of PLP enzymes, would provide information on cofactor orientation within the crystal. This is of particular importance since it has been established for aspartate aminotransferase that the external aldimine (III in Scheme I) has a markedly different orientation in the molecule than do the internal aldimines I or **II**.[6-10]

The combination of refined structural models obtained from X-ray crystallography and linear dichroism data on the same crystal will, in favorable cases, both confirm that the TDM direction is parallel to the cofactor's pyridine ring, and give an experimental value for the TDM direction in the ring plane.[6,9] In the protein crystal the separation between the chromophores of different molecules is large, and therefore the "oriented gas" approximation[11] can be used in the evaluation of the TDM. However, such combined X-ray and linear dichroism data are rather rare, because often crystals are not suitable for linear dichroism measurements because of either an inappropriate space group or their physical dimensions, or both,[11] the triclinic crystals of the unliganded forms of chicken mitochondrial AspAT (mAspAT) being a noteworthy example of these problems.[9]

Chicken mAspAT provides a unique system for such studies since both X-ray and linear dichroism data are available from crystals of orthorhombic symmetry for a number of different enzyme forms that are good models of catalytic intermediates.[6,8,9,12-15] The PLP enzyme at both high and low pH (I and II in Scheme I) and the PMP enzyme (IV in Scheme I) all have the open structure which the enzyme assumes in the absence of ligands. They crystallize in the triclinic space group P1[14,16,17] and will be referred to as HPH, LPH, and PMP, respectively. The Michaelis-type noncovalent complex of PLP enzyme with maleate and the covalent PLP enzyme inhibitor complex with 2-methylaspartate exhibit the closed structure in which the ligand is completely surrounded by the protein. Crystals of the closed structure belong to the orthorhombic space group $C222_1$.[8,14,15] Many other AspAT structures have been reported by other groups (see ref 8 for a review and additional references).

To obtain additional insight into the assignment and interpretation of PLP-AspAT spectra, theoretical calculations have been reported.[18-20] However, most of the results published for these spectra have been based on the Pariser-Parr-Pople (PPP) π-electron-only method and have included explicitly only the cofactor in its different forms. It is possible to apply this method to hydrogen-bonding effects by careful adjustment of the parameters for the N and O atoms assumed to be proton donors or acceptors. However, the fact that hydrogen atoms are not explicitly included in the π-electron methods inevitably requires making assumptions about the protonation state of certain atoms and about nonnegligible interactions between PLP and neighboring amino acid residues. Because of this, it is not possible to analyze the way in which the cofactor's nearest protein environment affects its spectrum. Empirical methods have also been developed to treat hydrogen bonding in the study of the spectra of cofactors in proteins.[21]

We describe here results obtained from the application of an all-valence-electron method to protein spectra for a number of forms of the PLP-mAspAT enzyme, using the crystal structures reported by Jansonius and co-workers (see above). First, we wish to test the applicability of the method to PLP enzyme systems and to determine if the results obtained are comparable to available experimental data for structures which are known. This will establish whether the method can subsequently be used to predict

(6) Vincent, M. G.; Picot, D.; Eichele, G.; Jansonius, J. N.; Kirsten, H.; Christen, P. In *Chemical and Biological Aspects of Vitamin B_6 Catalysis*; Evangelopoulos, A. E., Ed.; A.R. Liss Inc.: New York, 1984; Part B, pp 233-243.

(7) Arnone, A.; Christen, P.; Jansonius, J. N.; Metzler, D. E. In *Transaminases*; Christen, P., Metzler, D. E., Eds.; John Wiley: New York, 1985; pp 326-357.

(8) Jansonius, J. N.; Vincent, M. G. In *Biological Macromolecules and Assemblies*; Jurnak, F. A., McPherson, A., Eds.; John Wiley: New York, 1987; Vol. 3, pp 187-285.

(9) Picot, D. Ph.D. Dissertation, University of Basel, Switzerland, 1986.

(10) Makarov, V. L.; Kochkina, V. M.; Torchinsky, Y. M. *Biochim. Biophys. Acta* **1981**, *659*, 219-228.

(11) Hofrichter, J.; Eaton, W. A. *Annu. Rev. Biophys. Bioeng.* **1976**, *5*, 511-560.

(12) Ford, G. C.; Eichele, G.; Jansonius, J. N. *Proc. Natl. Acad. Aci. U.S.A.* **1980**, *77*, 2559-2563.

(13) Kirsch, J. F.; Eichele, G.; Ford, G. C.; Vincent, M. G.; Jansonius, J. N.; Gehring, H.; Christen, P. *J. Mol. Biol.* **1984**, *174*, 497-525.

(14) Jansonius, J. N.; Eichele, G.; Ford, G. C.; Picot, D.; Thaller, C.; Vincent, M. G. In *Transaminases*; Christen, P., Metzler, D. E., Eds.; John Wiley: New York, 1985; pp 110-138.

(15) Picot, D.; Sandmeier, E.; Thaller, C.; Vincent, M. G.; Christen, P.; Jansonius, J. N. *Eur. J. Biochem.* **1991**, *196*, 329-341.

(16) Gehring, H.; Christen, P.; Eichele, G.; Glor, M.; Jansonius, J. M.; Reimer, A.-S.; Smit, J. D. G.; Thaller, C. *J. Mol. Biol.* **1977**, *115*, 97-101.

(17) McPhalen, C. A.; Vincent, M. G.; Jansonius, J. N. *J. Mol. Biol.* **1992**, *225*, 495-517.

(18) Morozov, V. Y. In *Vitamin B_6. Pyridoxal Phosphate*; Dolphin, D., Poulson, R., Avramovich, O., Eds.; John Wiley: New York, 1986; Part A, pp 131-180.

(19) Savin, P. S. In *Physico-Chemical Problems of Enzymatic Catalysis*; Torchinsky, Yu. M., Ed.; Nauka: Moscow, 1984; pp 69-83.

(20) Song, P. S. Private communication to E.L.M., 1980.

(21) Warshel, A.; Lappicirella, A. *J. Am. Chem. Soc.* **1981**, *103*, 4664-4673. Warshel, A.; Russell, S. T. *Q. Rev. Biophys.* **1984**, *17*, 283-422.

spectra which are not available. Secondly, we wish to determine how sensitive the predicted spectrum is to structural changes, e.g., those observed in the catalytic reaction step from internal to external aldimine. Thirdly, it would be useful to establish a basis for explaining and predicting shifts of the absorption bands of different catalytic intermediates, such as the variation of wavelength between 325 and 360 nm which has been observed for the unprotonated PLP aldimine.[22]

The calculations described here have been carried out on model complexes of the cofactor forms I, II, and IV in Scheme I (HPH, LPH, and PMP, respectively), with selected residues in the active site of mAspAT. The term "model complex" is used here for a limited set of atoms chosen from the groups which interact with the coenzyme. The residues included in the calculations, their H-bonding patterns, and the groups which are used as models for them are shown in Scheme III. Tyrosine 225 and asparagine 194 are both hydrogen-bonded to the ionized 3-hydroxyl group of the cofactor pyridine ring. Aspartate 222 is H-bonded to the protonated N1 of the pyridine ring, to a water molecule, and to histidine 143, which is further H-bonded to serine 139. Tryptophan 140 may undergo π-stacking interactions with the cofactor pyridine ring. The PMP complex includes, in addition, a model for the charged lysine 258 ϵ-amino group. (For stereodiagrams see refs 8 and 17.)

The results presented below illustrate the effects on the predicted spectra of interactions between the cofactor and the residues shown in Scheme III. This requires no special parametrization; i.e., in the method used here, the parameters are defined for a given atom and are independent of its protonation state, in contrast to standard π-electron methods. Thus, for example, the parameters for the aldimine N, protonated or not, are the same as those used for the protonated pyridine N1 and the neutral asparagine N. This clearly eliminates the need for any a priori assumptions about the existence or relative strengths of interactions and, in fact, permits the evaluation of their importance in the different enzyme forms.

Methods

1. Calculations. The model complexes have been simplified by using a single methyl group for the four methylene groups in the side chain of Lys258, and by substituting OCH_3 for the PO_4^{2-} group at C5′. These are probably not significant modifications, since the phosphate group has no influence on the spectra,[2] and indeed the calculations reported here indicate no contribution of the methoxy group to the molecular orbitals which are responsible for the excitations discussed below.

a. Addition of Hydrogen Atoms to Crystallographic Structural Data. The geometries for the C, N, and O atoms used as input to the spectral calculations are taken from the X-ray structures[17] that have been deposited with the Brookhaven Protein Data Bank[23] (Code Nos. 7AAT, 8AAT, 9AAT). Hydrogen atoms are then added as follows: Distances, valence angles, and torsion angles of the C, N, and O atoms are generated from the crystal data, and hydrogen atoms are added using standard bond lengths and valence angles.[24] The hydrogen positions are then optimized using the AM1 Hamiltonian contained in the AMPAC program;[25] the Cartesian coordinate optimization option has been used with the coordinates of the C, N, and O atoms fixed at their crystallographic values. The Fletcher–Powell variable matrix minimization option has been used for all H-atom optimizations except that of the enolimine, where the protonation of the O3′ gives a structure which represents a local minimum, and the Bartel gradient minimization option was employed.

b. SCF–CI Calculation of Spectra. The spectral calculations reported here are based on the semiempirical self-consistent-field (SCF) INDO method,[24] extended to the prediction of excited states by Ridley, Bacon, and Zerner.[26,27] Our program has been independently developed from the CNDO/2-3R program,[28] and the parameters of the Zerner group were modified in an earlier application to optimize the prediction of both singlet and triplet excited states in small model compounds such as benzene, pyridine, and benzaldehyde. These parameters are used without further modification for the present application and are given in Table I. Only one-electron excitations among the canonical SCF wave functions using the virtual orbital approximation have been treated in the configuration interaction (CI). The energies of the excitations from the 50 highest occupied MO's and the 50 lowest unoccupied (virtual) MO's were scanned, and those below a specified cutoff were included in the CI; the cutoff energy was increased until the predicted wavelength changed by less than 1 nm for an additional 25 excitations. Convergence was attained when the excitation energy reached 10 to 11 eV. The number of configurations included varied from about 50 for PLP alone to about 350 for the seven-residue complexes.

Table I. INDO Parameters Used in the Present Work (eV)

atom	I_s	I_p	β	F^0	G^1[a]	F^2[a]
H	13.06			-9.0	10.5	
C	19.44	10.67	-18.5	8.5	7.2846	4.7271
N	25.58	13.19	-27.5	9.5	9.4158	5.9607
O	32.38	15.85	-35.5	12.5	11.8158	7.2494

[a] Theoretical values as given in ref 23.

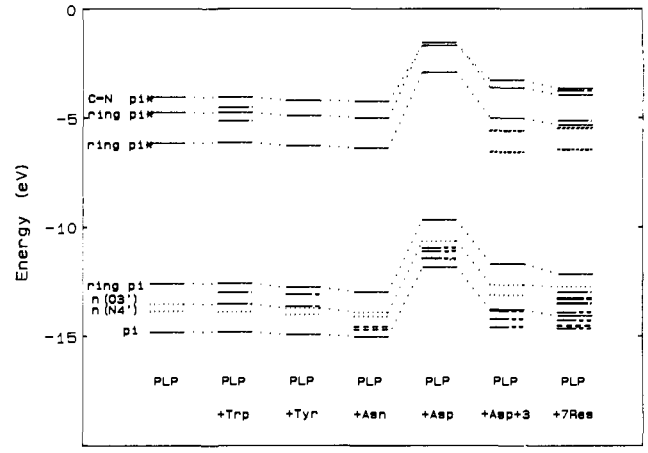

Figure 1. Molecular orbital energy level correlation diagram for higher energy occupied and lower energy unoccupied orbitals of HPH, the unprotonated aldimine of PLP–mAspAT, showing the effects of different residues. PLP molecular orbitals are labeled according to their type, and the change in energy for different complexes is shown by a dotted line: (—) PLP π; (···) PLP n; (—·) Trp140; (—-) Tyr225; (---) Asn194; (—··) Asp222.

2. Solution Spectra. Absorption spectra of mAspAT in sodium phosphate buffered solution were recorded on a Uvikon 860 spectrophotometer (Kontron Instruments). The protein concentrations were determined from the absorbance at 279 nm and were found to be 0.75 mg/mL for the internal aldimines and 0.73 mg/mL for the PMP form. The pH values were 8.5 for the unprotonated aldimine, 4.5 for the protonated form, and 7.5 for the PMP enzyme. The spectra were computerized using the AppleScanner and digitized using the Macintosh program Image. No interpolation of the digitized data was employed.

3. Lognormal Distribution Curves. The solution spectra have been deconvoluted with lognormal functions.[29] In addition, predicted spectra have been simulated using the calculated wavelengths and intensities as parameters and fitting them to the functions found for the appropriate bands in the experimental spectra.

Results and Discussion

The SCF–CI calculations have been carried out for two enzyme forms of PLP–mAspAT and one of PMP-mAspAT. For the two internal aldimines HPH and LPH, the calculations have been done first on isolated PLP; then on PLP plus a single residue, either tryptophan or one of the three different H-bonding groups; and, finally, PLP plus seven residues from the active site. These models

(22) Kallen, R. G.; Korpela, T.; Martell, A. E.; Matsushima, Y.; Metzler, C. M.; Metzler, D. E.; Morosov, Y. V.; Ralston, I. M.; Savin, F. A.; Torchinsky, Y. M.; Ueno, H. In *Transaminases*; Christen, P., Metzler, D. E., Eds.; John Wiley: New York, 1985; pp 37–108.

(23) Bernstein, F. C.; Koetzle, T. F.; Williams, G. J. B.; Meyer, E. J., Jr.; Brice, M. D.; Rogers, J. R.; Kennard, O.; Shimanouchi, T.; Tasumi, M. *J. Mol. Biol.* **1977**, *112*, 535–542.

(24) Pople, J. A.; Beveridge, D. L. *Approximate Molecular Orbital Methods*; McGraw-Hill: New York, 1970.

(25) (a) Dewar, M. J. S.; Zoebisch, E. G.; Healy, E. F.; Stewart, J. J. P. *J. Am. Chem. Soc.* **1985**, *107*, 3902–3909. (b) AMPAC: Austin Method 1 (QCPE 506); Version 1.0. Dewar Research Group. Stewart, J. J. P. *QCPE Bull.* **1986**, *6*, 24.

(26) Ridley, J.; Zerner, M. C. *Theor. Chim. Acta* **1973**, *32*, 111–134.

(27) Bacon, A. D.; Zerner, M. C. *Theor. Chim. Acta* **1979**, *53*, 21–54.

(28) (a) Hase, H. L.; Schweig, A. *Theor. Chim. Acta* **1973**, *31*, 215–220. (b) Hase, H. L.; Schweig, A. *QCPE* **1974**, *11*, 261.

(29) Siano, D. B.; Metzler, D. E. *J. Chem. Phys.* **1969**, *51*, 1856–1861.

Table II. Calculated Wavelengths (λ), Intensities (ε), and Directions of the Transition Dipole Moment Vectors (ω) to the N1–C4 Axis of the PLP Pyridine Ring for the Unprotonated and Protonated Internal Aldimines

	1. HPH: unprotonated aldimine N calculated transitions			2. LPH: protonated aldimine N					
				calculated transitions			simulated spectrum[a]		
species	λ (nm)	ε (M^{-1} cm^{-1})	ω (deg)	λ (nm)	ε (M^{-1} cm^{-1})	ω (deg)	λ (nm)	ε (M^{-1} cm^{-1})	ω (deg)
a. PLP	394.8	11986	47	473.0	3226	45	428	15439	48
	374.0	66	−51	425.5	13220	49			
b. PLP + Trp140	393.0	10340	47	526.9	232	66	417	11119	49
	368.9	62	−27	473.3	4521	44			
				446.5	1891	51			
				411.4	7927	47			
c. PLP + Tyr225	391.2	10441	50	463.6	4127	47	424	13445	50
	369.0	1302	40	432.6	4715	52			
	314.8	427	78	414.8	6720	51			
				351.8	146	58			
d. PLP + Asn194	381.0	12672	47	455.9	6224	47	418	14140	49
	353.7	117	19	413.9	10400	51			
	315.7	425	76	306.6	2	24			
e. PLP + Asp222	365.9	12600	46	472.2	4876	39	441	13725	47
	334.4	48	18	434.8	10075	52			
	304.0	352	76	375.5	705	0			
				314.4	115	−8			
f. PLP + Asp222 + Wat + His143 + Ser139	405.7	2		455.9	6085	43	426	13564	48
	373.6	12241	45	419.6	9409	51			
g. PLP + Tyr225 + Asp222 + Asn194	349.2	12620	49	454.0	8197	44	435	12453	48
	312.0	424		422.9	5769	62			
				371.8	671	16			
h. PLP + Trp140, Asp222, Asn194, Tyr225, Wat, His143, Ser139	355.8	10187	48						
	317.8	447	41						
	307.8	330	−75						
aldimine N protonated				440.3	9829	48	437	10867	51
				400.1	2430	62			
				365.2	546	25			
				347.8	114	66			
O3′ protonated				387.1	330	−8	312	9132	58
				325.6	2762	75			
				312.5	4579	59			
				299.1	166	−62			
				298.5	1436	−34			
i. PLP + 7 res, as above; His143 neutral	347.4	10612	49	458.2	8329	45	447	10523	49
				429.0	2911	71			
				402.4	835	37			
				373.6	551	20			
				349.2	531	53			
				343.1	26	73			
				326.5	19	17			

[a] The parameters for bandwidth and skewness used in the simulation are given in Table V.

Table III. Wavelengths of Maximum Absorption (λ), Intensities (ε), and Directions of the Transition Dipole Moments (ω) for Pyridoxal 5′-Phosphate Internal Aldimine Unprotonated (HPH) and Protonated (LPH), and Pyridoxamine Phosphate (PMP), Calculated Using Crystal Structures, with Observed Values and Results of Earlier Calculations Included for Comparison

	calculated, this work			observed		earlier calculations	
enzyme form	λ (nm)	ε (M^{-1} cm^{-1})	ω (deg)	λ (nm)[a]	ω (deg)[b]	ω (deg)[c]	ω (deg)[d]
HPH: PLP + 7 res	356	10187	48	355	49	36	52
LPH: PLP + 7 res	437	10687	51	433	40	39	55
	312	8665	58	328			
PMP: PMP + 7 res	375	26	27				
	354	8772	60	331	53	49	
PMP + 8 res	348	9348	65	331	53	49	

[a] Solution spectra ±2 nm; see Table IV and Figures 3a and 4a. [b] ±10 deg; ref 9. [c] Reference 19. [d] Reference 20.

are shown in Scheme III, and the calculated values of wavelengths, intensities and TDM directions for the lower energy transitions are listed in Table II. The results of calculations on the two internal aldimines and the PMP are compared with observed values and the results of earlier calculations in Table III.

1. HPH: High-pH Form, Unprotonated Internal Aldimine. The results of the SCF calculations are summarized in the molecular orbital (MO) energy level correlation diagram in Figure 1, and the wavelengths, intensities, and angles ω formed by the TDM to the N1-C4 axis (see Scheme II) obtained from the CI calculations are given in Table II. For the isolated unprotonated PLP aldimine (Table II, 1a), the SCF calculations predict that the PLP ring π MO is the highest occupied (HOMO), with the O3′ lone pair orbital, $n_{O3'}$, the second highest occupied (HOMO−1). The two lowest unoccupied orbitals (LUMO, LUMO+1) are ring π* MO's, with the C=N π* at somewhat higher energy. The aldimine π* orbital is distinct from that of the ring owing to the noncoplanarity of these groups found in the crystal structure, with

a torsion angle[17] χ(C3–C4–C4′–N4′) of 76°. For PLP paired with the residues Trp140 (1b), Tyr225 (1c), or Asn194 (1d), the PLP orbital energies vary only slightly (see Figure 1). In 1b and 1c, two π MO's of tryptophan or tyrosine are predicted to have an energy between those of the PLP ring π and the $n_{O3'}$; in addition, there is some mixing of the tyrosine π MO's with the PLP $n_{O3'}$ orbital. With Asn194, the highest energy MO of asparagine lies below the PLP $n_{O3'}$.

The species 1a, 1b, 1c, and 1d (Table II) are all bipolar neutral, the −1 charge on O3′ being balanced by the +1 charge on the protonated N1. However, in the complex 1e, PLP–Asp222, the aspartate group introduces a net charge of −1. This raises all the MO energies by about 3 eV relative to those of the neutral species. The aspartate MO's are all at slightly lower energy than the π and $n_{O3'}$ of PLP itself, but it is found that the PLP $n_{O3'}$ mixes extensively with the aspartate O lone pair orbitals, leading to three MO's with energies below the PLP ring π orbital and above the aspartate COO^- π orbital. This ordering of MO's is strongly affected by the inclusion of the groups H-bonded to Asp222, that is, a water molecule and the His143–Ser139 H-bonded pair (1f). These modulate the charge density on the aspartate and lower substantially the aspartate MO energies relative to those of PLP, so that the essentially pure PLP $n_{O3'}$ is again HOMO-1. With the inclusion of seven residues (1h), all the ligand MO's lie below both the π and the $n_{O3'}$ of PLP. The LUMO and LUMO+1 are predicted to be histidine π* MO's.

The spectrum calculated for the isolated PLP internal aldimine is rather simple, consisting of the intense π → π* transition at 395 nm, and the $n_{O3'}$ → π* transition at 374 nm with a negligible intensity (see Table II). These predicted wavelengths are not comparable with experimental data since they are for PLP in vacuo. Any π-stacking interaction that may exist between the PLP and the tryptophan rings has very little effect on the spectrum, giving a shift of less than 2 nm to the π → π* transition of PLP. Interaction with Tyr225 or Asn194 shifts the π → π* transition by 4 and 14 nm, respectively, to shorter wavelength. These shifts are indicative of decreased polarization in the excited state.[30] Comparison of the π and π* wave functions shows a shift of charge from O3′, negatively charged in the ground state, to N1 and C2, essentially neutral in the ground state. The effect of interaction with Asp222 is more marked: the π → π* transition is now predicted at 366 nm, a blue shift of 29 nm relative to the isolated PLP aldimine. This large shift in the predicted transition energy is reduced to 21 nm when the groups H-bonded to aspartate are included (1f in Table II). Simultaneous inclusion of the three groups H-bonded to N1 or O3′ (1g) leads to a blue shift of 45 nm, which is the sum of the three individual effects, with the predicted absorption maximum at 349 nm.

When all seven residues are included with PLP (1h), the spectrum for the unprotonated aldimine is predicted to have the PLP ring π → π* transition at 356 nm, with a net shift of 39 nm due to the combined effects of the different interactions, which appear to be additive. This prediction agrees to within 1 nm with the observed λ_{max} (see Table III). Although histidine MO's are predicted to be the LUMO and LUMO+1, excitations from the highest energy occupied MO's to these orbitals have negligible intensities. Electronic excitation from the $n_{O3'}$ to the PLP π* gives a second transition at 318 nm, and excitations from tryptophan π to the π* of PLP and the π* of the C=N group lead to a transition at 308 nm, both very weak. Results are given also for the spectrum predicted if His143 is assumed to be uncharged (1i), with loss of H-bonding to Asp222. Here the shift of 8 nm to shorter wavelength is about the same as the difference in λ_{max} between species 1e and 1f. Comparison of this predicted λ_{max} with that of 1h and with the observed value indicates that His143 is likely to be charged.

2. LPH: Low-pH Form, Protonated Internal Aldimine. The SCF results for the protonated form of PLP are summarized in the MO energy level diagram in Figure 2, and the CI results for the calculated transitions and the simulated spectra are given in Table II. In LPH the aldimine group is parallel to the ring, with an observed torsion angle[17] χ(C3–C4–C4′–N4′) of 0°, and the π and π* MO's contain contributions from both groups. In PLP (2a) the HOMO is the π MO involving predominantly the ring, with the $n_{O3'}$ somewhat below this in energy. The LUMO and LUMO+1 are combinations of the ring and the (C=N) π* orbitals. Interactions between PLP and Trp140 (2b) or Tyr225 (2c) have little effect on the PLP MO energies (see Figure 2). However, two occupied π MO's of tryptophan or tyrosine are higher in energy than the PLP π. The energies of the PLP MO's decrease slightly with the introduction of Asn194 (2d), and two MO's of asparagine have energies between those of the PLP π and $n_{O3'}$.

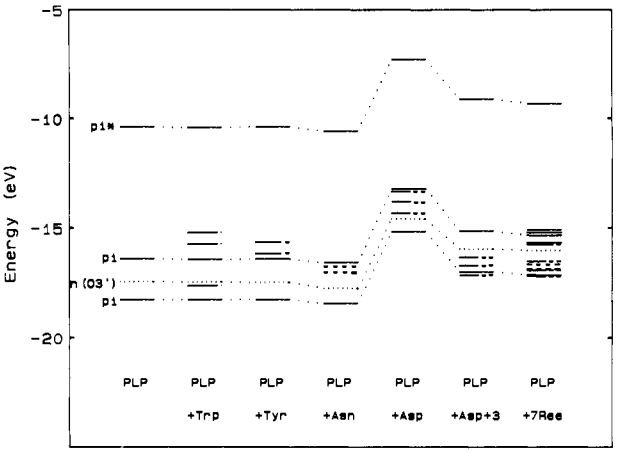

Figure 2. Molecular orbital energy level correlation diagram for higher energy occupied and lower energy unoccupied orbitals of LPH, the protonated aldimine of PLP–mAspAT, showing the effects of different residues. PLP molecular orbitals are labeled according to their type, and the change in energy for different complexes is shown by a dotted line: (—) PLP π; (···) PLP n; (—·) Trp140; (— -) Tyr225; (- - -) Asn194; (— - -) Asp222.

These four species all have a net charge of +1, due to the protonated aldimine N. In contrast, protonated PLP plus Asp222, 2e, gives a bipolar neutral complex, and the energies of all the MO's are increased, as already seen for the unprotonated aldimine. In addition, the MO's of 2e show appreciable interaction between the $n_{O3'}$ and the lone pair orbitals of the aspartate. Inclusion of the water molecule and the His143–Ser139 pair which are H-bonded to Asp222 (2f) strongly alters the predicted spectrum, since they modulate the charge density on the carboxylate group and lower its MO energies, bringing them below the PLP $n_{O3'}$ energy. Inclusion of all seven residues, 2h, leads to mixing of the PLP HOMO π with two π MO's of tryptophan and the higher energy π MO of tyrosine, the four highest energy MO's of the complex being combinations of these in differing proportions (Figure 2).

The predicted spectrum of the protonated aldimine of PLP, 2a, is more complex than that of the unprotonated form. Two excitations of about the same energy are calculated in the wavelength region of interest, an intense π → π* and a very weak $n_{O3'}$ → π* excitation. These mix extensively in the CI, giving rise to two transitions, in contrast to the single transition predicted for the unprotonated aldimine (see above). For 2a the two lowest energy transitions occur at 473 nm and at 426 nm. The former is of moderate intensity and more n → π* in nature, whereas the latter is of strong intensity and more π → π* in nature. The simulated spectrum obtained using lognormal functions gives the absorption maximum at 428 nm (see Table II), with a shoulder on the long-wavelength side.

Although the π-stacking interaction between PLP and Trp140 (2b) had little effect on the MO energies of the former, there are pronounced effects on the spectrum. The mixing of PLP and tryptophan π → π* excitations with the $n_{O3'}$ → π* leads now to four predicted transitions of varying intensity in the region of interest. The simulated spectrum (see Table II) has λ_{max} at 417

(30) Jaffe, H. H.; Orchin, M. *Theory of Ultraviolet Absorption Spectroscopy*; John Wiley: New York, 1962; p 186 ff.

nm, a shift of 11 nm to shorter wavelength relative to the isolated PLP, with a broad shoulder at about 475 nm. If hydrogen-bonding interactions with Tyr225 or Asn194 are considered (2c and 2d, respectively), the predicted transitions undergo a blue shift, and the simulated spectra exhibit absorption maxima at 424 and 418 nm, respectively. As noted above for the unprotonated aldimine, this shift indicates a decreased polarization of the excited state. In the complex of PLP with Tyr225, the second predicted transition is due predominantly to tyrosine $\pi \rightarrow$ PLP π^* excitations, although there is appreciable mixing of these with the PLP excitations. In the complex of PLP with Asn194, the spectrum is more like that predicted for isolated PLP, with the asparagine to PLP π^* transitions occurring at relatively high energy and low intensity, and with essentially no mixing with other excitations. The calculated spectrum resulting from H-bonding interactions with Asp222, 2e, predicts that charge-transfer (CT) excitations from aspartate oxygen lone pair orbitals to PLP π^* interact strongly with both the $\pi \rightarrow \pi^*$ and $n \rightarrow \pi^*$ of the PLP, resulting in a marked red shift of the simulated spectrum of 13 nm (see Table II, 2e). This is the only red shift found in all the interactions studied, and contrasts with the blue shift found when Asp222 interacts with the unprotonated aldimine. In the latter, the interaction appears to be essentially H-bonding in the ground state. In the protonated form here, the CT interactions in the excited state appear to outweigh the H-bonding interactions of the ground state. However, similar to the case of the unprotonated aldimine discussed in section 1 above, inclusion of the groups H-bonded to the aspartate (2f) strongly modulate this shift, leading to a net shift of 2 nm to shorter wavelength relative to isolated PLP. This is due to charge-transfer effects partially neutralizing the −1 charge on the carboxylate and a lowering in energy of its MO's. If the three groups H-bonded to N1 or O3′ of PLP are included (2g), the simulated spectrum has an absorption maximum at 435 nm.

The predicted spectrum of PLP together with the seven residues (2h) has a λ_{max} of 437 nm, as compared to 433 nm observed experimentally (see Table III). This is a net shift of 9 nm to longer wavelength relative to that of PLP itself and is due primarily to the strong mixing of the tryptophan and PLP MO's in the ground state. Thus the effects of the different residues are not additive in the case of the protonated aldimine, in contrast to that of the unprotonated form discussed above. The prediction for the tautomeric enolimine, with O3′ rather than the aldimine N protonated, has a λ_{max} at 312 nm, about 16 nm shorter than observed experimentally (see Table III and section 4 below). If His 143 is assumed to be neutral (2i), with loss of H-bonding to Asp222, the absorption maximum is predicted to shift by 10 nm to the red, compared to the 15-nm difference in λ_{max} for the species 2e and 2f. Comparison of this predicted λ_{max} with that of 2h and with the observed value indicates that His143 is likely to be charged, as found for HPH.

3. PMP: Pyridoxamine Phosphate Form of mAspAT. The calculations on the PMP spectrum have been done with the seven residues shown in Scheme III and, in addition, Lys258 with a charged ϵ-amino group. The calculated results are compared to observed values in Table III. As in the case of HPH, the spectrum has its origin in a single excitation, the PMP $\pi \rightarrow \pi^*$.

The predicted spectrum for PMP is not in as good agreement with experiment as those of HPH and LPH. A comparison of isolated PMP with isolated, unprotonated PLP shows a wavelength difference of only 1 nm, with the HOMO and LUMO orbitals being very similar both in energy and in the atomic orbital coefficients. This is not surprising, since the only structural difference between the two isolated chromophores is the saturated amine of PMP as compared to the imine group of PLP. Since both these groups are almost perpendicular to the pyridine ring plane, neither contributes to the HOMO or LUMO orbitals which are involved in the predicted transition. Inclusion of the seven residues gives a calculated wavelength difference of only 2 nm between PMP and HPH (Table III). The addition of charged Lys258 H-bonding to PMP shifts the predicted transition 6 nm to shorter wavelength. The crystallographic structural data[17] show that all the H-bonding distances between the O3′ or N1 with Tyr225, Asn194, and Asp222 are shorter in PMP than in HPH, which should lead to stronger interactions and consequently larger blue shifts in the predicted spectrum, as observed experimentally. This has not been found in the calculations.

Table IV. Parameters Used in Fitting Lognormal Functions to Solution Spectra

enzyme form	band	λ_0 (nm)	ϵ_0 (M^{-1} cm^{-1})	width (cm^{-1})	ρ
HPH	1	430	400	4200	1.5
	2	355	7140	4800	1.6
	3	320	610	5000	1.6
	4	280	16660	5000	1.5
LPH	1	433	6280	4200	1.7
	2	358	970	4500	1.7
	3	328	2290	5000	1.6
	4	280	30400	5000	1.5
PMP	1	430	180	4200	1.6
	2	355	550	4800	1.6
	3	331	7920	3500	1.6
	4	280	18010	5000	1.5

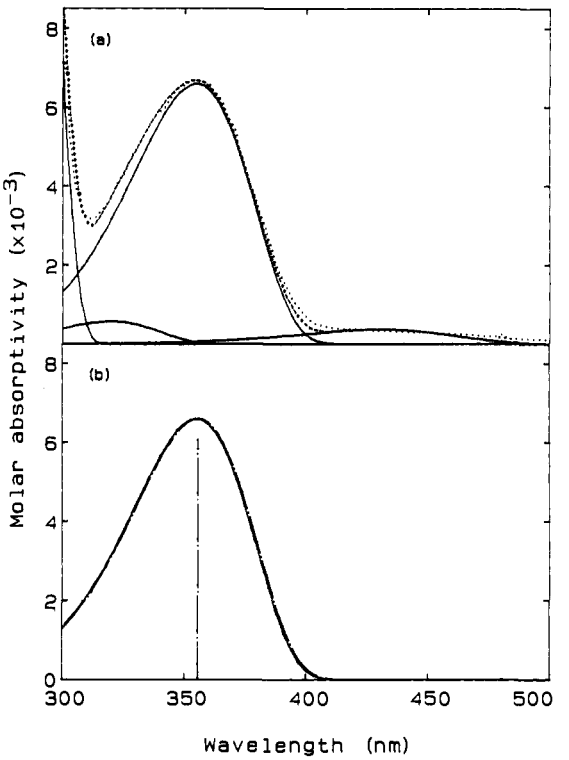

Figure 3. (a) Lognormal distribution functions (—) and their sum (- - -) fit to the solution spectrum (···) of HPH using the parameters in Table III. (b) Calculated spectrum (- - -) simulated using the lognormal function defined by the predicted λ_0 (- - -) and other parameters given in Table IV for HPH, compared with band 2 (—) of the solution spectrum in (a).

4. Comparison of Calculated and Observed Spectra. In order to compare the results of the calculations with experiment, especially in the case of LPH where multiple transitions are predicted, solution spectra have been fitted with lognormal distribution curves for which the parameters are given in Table IV. These parameters for chicken mAspAT are within about 10% of the values published for pig mAspAT.[22]

Figure 3a shows the lognormal functions fitted to the solution spectrum of the unprotonated internal aldimine HPH. Four functions have been used, and, although the fit is not perfect at the long-wavelength, low-intensity region of the spectrum, additional functions have not been included. The main absorption band 2, with λ_0 = 355 nm, is due to the unprotonated aldimine, and the low-intensity band 1 at longer wavelength is assigned to the protonated form. The origin of the weak band 3 with λ_0 = 320 nm is not known, although this band has been previously

Table V. Parameters Used in Fitting Calculated Transitions to Lognormal Functions Found for Solution Spectra

enzyme form	band	λ_0 (nm)	ϵ_0 (M^{-1} cm^{-1})	width (cm^{-1})	ρ
HPH	2[a]	355.8	7140	4800	1.6
LPH	1[b]	436.3	5780	3300	1.42
		396.1	1430	3300	1.42
		361.1	320	3300	1.42
		343.8	70	3300	1.42
	3[c]	403.1	100	4000	1.7
		341.6	820	4000	1.7
		328.5	1370	4000	1.7
		315.1	50	4000	1.7
		314.5	430	4000	1.7
PMP	3[d]	347.8	7920	3500	1.6

[a] λ_0 from Table II, 1h; ϵ scaled by 0.7. [b] λ_0 from Table II, 2h, shifted by −4 nm; ϵ scaled by 0.6. [c] λ_0 from Table II, 2h shifted by 16 nm; ϵ scaled by 0.3. [d] λ_0 from Table III; ϵ scaled by 0.8.

observed.[31] The very intense band 4 with λ_0 = 280 nm is found in the spectra of all the enzyme forms due to absorption by the numerous aromatic rings of the protein. It is the intensity of this absorption band which provides the means of determining the protein concentration and hence of evaluating the extinction coefficients ϵ given in Table IV.

The unprotonated PLP interacting with seven residues, species 1h in Table II, has a predicted λ_{max} of 356 nm, a single intense transition in the spectrum for $\lambda > 300$ nm, in excellent agreement with the λ_0 value for band 2 of HPH in Table IV. In comparing the calculated spectrum with band 2 of the experimental spectrum, the predicted extinction coefficient of 10 187 M^{-1} cm^{-1}, given in Table II, 1h, has been scaled by a factor of 0.7 (see Table V). This is within a reasonable limit, since semiempirical methods yield intensities which can be in error by as much as a factor of 2. The predicted spectrum is simulated with a lognormal curve using the parameters given in Table V and is compared with band 2 of the solution spectrum in Figure 3b. Since the value of λ_0 differs by less than 1 nm, it is not surprising that the two curves agree very well.

A more critical comparison of the calculated results with experiment is afforded by the protonated aldimine, since Table II, 2h, shows that there are a number of transitions predicted for the long-wavelength region. The solution spectrum is shown in Figure 4a, with the lognormal functions fitted with the parameters given in Table IV. The long-wavelength band 1, with λ_0 = 433 nm, is due to the cofactor with the aldimine N protonated.[31] Band 2 can be assigned to the unprotonated aldimine, since it was found in a series of spectra from pH 8.5 to 4.5 with decreasing intensity. Band 3, which is more intense here than in the HPH spectrum of Figure 3a, has been suggested to be due to the tautomeric enolimine, with O3′ rather than the aldimine N protonated.[31] In comparing the predicted transitions given in Table II with experiment, the wavelengths for the protonated aldimine have been shifted by −4 nm and the intensities have been scaled by a factor of 0.6. For the enolimine, the wavelengths from Table II have been shifted by 16 nm and the intensities have been scaled by a factor of 0.3. The shifted λ and scaled ϵ values are given together with the bandwidth and skewness parameters in Table V. Although it would be quite reasonable to expect that the different calculated transitions could have different bandwidth and skewness parameters, this would give a large number of degrees of freedom in the fitting, so we have chosen the simpler procedure of assuming them all the same. As can be seen in Figure 4b, the shapes of the simulated and the experimental bands match quite well. In the long-wavelength band 1, inclusion of the two weakest of the four predicted transitions is important for obtaining a good fit at the short-wavelength limit of the band. With regard to the enolimine, band 3, the shifting of predicted wavelengths by 16 nm is not unreasonable, since there is no way to determine exactly the position of the proton which has migrated from the aldimine N to O3′. The optimized position represents a local minimum in the ground-state energy surface. However, a small repositioning of this proton away from O3′ and toward the aldimine N shifts the predicted transitions to longer wavelength.

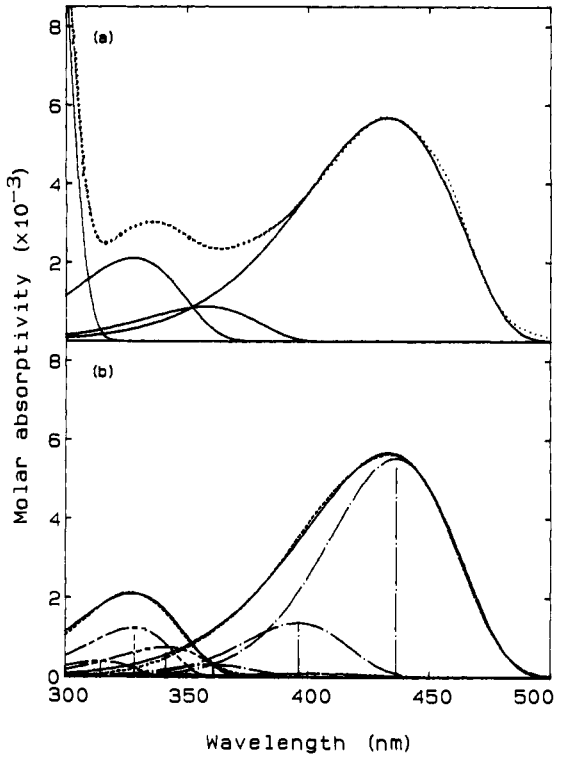

Figure 4. (a) Lognormal distribution functions (—) and their sum (---) fit to the solution spectrum (···) of LPH using the parameters in Table III. (b) Calculated spectrum (---) simulated using the lognormal function defined by the λ_0 for protonated internal aldimine (---) and for the enolimine (—--) with other parameters given in Table IV for LPH, compared with bands 1 and 3 (—) of the solution spectrum in (a).

5. Transition Dipole Moment Vectors. In the CI, the TDM's were evaluated with respect to the PLP ring plane, with N1 placed at the origin, C4 placed along the x axis, and C5 placed in the x,y plane. The TDM direction is measured by the angle ω (see Scheme II), the C2–C5 axis corresponding to a vector at +60°. The calculated intensities are those which would be observed if the incident radiation is perpendicular to the PLP ring. The angles ω given in Table II show that the TDM is not appreciably affected by the interactions with the neighboring side chains. The results given in Table III for HPH, LPH, and PMP agree within experimental error (±10°) with the measured values.

The results obtained here are in agreement with those of earlier calculations (Table III) in predicting a difference of only 3° in the TDM orientations of the protonated and unprotonated internal aldimines. This difference is too small to provide a clear answer to the question of whether the value of ω for LPH is larger or smaller than that for HPH. The calculations do indicate, however, that it is unlikely that the high pH form of the internal aldimine of mAspAT would have a TDM angle significantly smaller than that of the low pH form, such as the values of 10° and 27°, respectively, reported by Metzler et al. for cAspAT.[31]

Calculations done on the isolated cofactor with an energy-minimized geometry, in which the pyridine ring is more planar than is found in the X-ray refinements, indicate that the unprotonated aldimine could have a TDM angle of 10 to 20° larger than the protonated form, and that the PMP TDM angle could be substantially smaller than the calculated value given in Table III. Thus, the TDM orientation seems much more sensitive to small deviations in geometry than to H-bonding interactions.

6. Effect of Protonation State on Predicted Spectra. The predicted spectra have been found to be sensitive to proton positions, which are not available from X-ray experiments. The AM1 method, which has been parametrized particularly for the pre-

(31) Metzler, C. M.; Mitra, J.; Metzler, D. E.; Makinen, M. W.; Hyde, C. C.; Rogers, P. H.; Arnone, A. *J. Mol. Biol.* **1988**, *203*, 197–220.

diction of H-bonding,[25a] has been used for the geometry optimization. The correct prediction of the position of the proton bonded to N1 in LPH and PMP is dependent on the choice of residues included in the model. Initial geometry calculations with only the three residues directly H-bonded to PLP or PMP led to Asp222 being protonated at the expense of N1, although at physiological pH both N1 and Asp222 should be in the charged state. The uncertainty in the predicted position of the proton may be due to the absence of bulk solvent in the present model. However, the electronic structure of individual species is modulated primarily by direct interaction with their nearest neighbors, and field effects of more distant parts of the system are expected to be of lesser importance. If the water molecule and the His143–Ser139 pair which are found in the crystallographic structure to be H-bonded to Asp222 are included in the AM1 H-atom geometry optimization, as was done here, the position of the proton and thus the charged state of N1 and Asp222 are correctly predicted for both LPH and PMP.

A second protonation state which has been studied is that in which the PMP amino group rather than Lys258 is charged. AM1 predicted that the PMP would be protonated, which yields a calculated λ_{max} of 352 nm, 4 nm to the red of that for the structure with the Lys258 charged. Both are at longer wavelength than the observed value. For the protonation state with Asp222 and N1 neutral, the calculations yield a λ_{max} of 315 nm for Lys258 charged, and 330 nm with the PMP amine group charged. In both of these cases the simulated spectrum shows a prominent shoulder at the short-wavelength side of the main band which is not in agreement with the solution spectrum. Thus none of the spectra predicted for the four species considered gives good enough agreement with experiment to be conclusive.

7. Effect of Variation of Aldimine Conformation on Predicted Spectra and TDM's. Of interest are the relative effects of protonation of the aldimine N and of the coplanarity of the aldimine group with the pyridine ring on the absorption spectrum and the TDM direction. In the unprotonated form of the PLP internal aldimine with Lys258, the aldimine double bond lies almost perpendicular to the pyridine ring, with a torsion angle χ(C3–C4–C4′–N4′) of 76° (see section 1 above), while the protonated aldimine has a χ value of 0° (see section 2 above). That is, in the latter the aldimine group is parallel to the pyridine ring, but not strictly coplanar since C4′ is not quite in the ring plane.[17] Thus the combination of protonation and parallel orientation leads to an observed shift of about 90 nm in the absorption spectrum. Studies on PLP–oxime complexes have shown that the PLP–aminooxyacetate oxime absorbs at 383 nm[32] and that the oxime double bond is almost coplanar with the pyridine ring, with a torsion angle χ(C4′–N4′–O–R) of 16° (ref 33).

In view of these experimental data, it is of interest to study the effects on the absorption spectrum of the PLP form of mAspAT due to variation of the aldimine conformation as measured by the torsion angle χ. Calculations were carried out on both the protonated and unprotonated PLP aldimine, in the absence of interactions with any enzyme residues, that is, PLP in vacuo, as a function of χ, with no reoptimization of geometry at the various chosen values of χ. The results listed in Table VI should lend helpful insight into the effects of interest, even if they cannot be compared with experimental data. Although the protonated aldimine group would not be expected to rotate out of the ring plane because of the strong H-bond and charge interactions with O3′, it has been included for comparison.

At χ = 0°, both forms of the aldimine have about the same calculated transition energies for the most intense band. In the protonated form, interactions between the $\pi \rightarrow \pi^*$ and $n \rightarrow \pi^*$ excitations lead also to a transition of less intensity at longer wavelength which is predominantly $n \rightarrow \pi^*$. Both forms have a second $\pi \rightarrow \pi^*$ transition at about 285 nm, which does not interact with the lower energy excitations. When χ is increased to 30°, the $\pi \rightarrow \pi^*$ transition of the unprotonated form shifts slightly to shorter wavelength. In the protonated form there is a slight weakening of the interaction between the $\pi \rightarrow \pi^*$ and $n \rightarrow \pi^*$ excitations, and the transitions have reversed their relative energies, with the more intense, predominantly $\pi \rightarrow \pi^*$ transition now at longer wavelength. At χ = 60° the protonated aldimine is predicted to have two $\pi \rightarrow \pi^*$ transitions in the region of the spectrum with $\lambda > 300$ nm; neither interacts with the $n \rightarrow \pi^*$ excitations. The predicted spectrum for the unprotonated form shows a continuation of the gradual shifts to shorter wavelengths. At χ = 90°, the spectrum calculated for the unprotonated aldimine shows a further shift to shorter wavelength. For the protonated form, however, both $\pi \rightarrow \pi^*$ transitions move to longer wavelength, the first now having a greatly reduced intensity. The second $\pi \rightarrow \pi^*$ interacts strongly with the $n \rightarrow \pi^*$, leading to two predicted transitions separated by only 13 nm.

Table VI. Calculated Wavelengths (λ), Intensities (ϵ), and Direction of Transition Dipole Moment (ω) for the PLP Aldimine as a Function of the Torsion Angle C3–C4–C4′–N4′ (χ)

	HPH: unprotonated form				LPH: protonated form			
χ (deg)	origin[a]	λ (nm)	ϵ (M^{-1} cm^{-1})	ω (deg)	origin[a]	λ (nm)	ϵ (M^{-1} cm^{-1})	ω (deg)
0	n	562.0	114	−6	n+π	472.5	3375	44
	π	423.4	13895	36	π+n	423.8	13194	49
	n	344.6	484	16	π	283.4	7516	−51
	π	286.5	1492	−90				
30	n	467.6	445	37	π+n	463.6	9815	48
	π	420.4	13137	37	n+π	423.9	4205	53
	n	354.4	500	34	π	311.8	4648	−83
	π	286.2	2600	−67				
60	π	404.7	12476	44	π	455.2	6014	53
	n	384.8	114	21	n	391.6	10	−20
	n	335.8	558	59	π	362.0	9109	66
	π	282.6	7045	−43	n	303.5	140	49
90	π	389.0	11679	49	π	471.6	1913	35
	n	369.2	98	−83	π+n	380.9	6386	65
	n	303.8	432	78	π+n	368.1	6113	65
	π	279.6	9049	−56	n+π	329.2	7	37

[a] Origin(s) of electronic excitations, in order of decreasing contribution.

The differences in the calculated spectra of the two forms of the PLP aldimine are due primarily to the nature of the lowest unoccupied MO's, and involve the interaction, or lack of any, of the ring and C=N π^* orbitals. This interaction is at least partly due to protonation of the aldimine N, which leads to a net positive electronic charge of about +0.5 for the aldimine group, as compared to a small net negative charge of about −0.1 for that of the unprotonated form. In the latter there is essentially no interaction between the ring and the C=N orbitals at all values of χ considered; moreover, $n \rightarrow \pi^*$ excitations play essentially no role in its spectrum. In the predicted spectrum of the protonated aldimine, the $\pi \rightarrow \pi^*$ excitations interact with the $n \rightarrow \pi^*$ excitations, but the extent of this interaction varies inversely with the contribution of C=N to the π^* orbital. As χ increases, the C=N contribution to the LUMO increases and that to the LUMO+1 decreases. The HOMO–LUMO $\pi \rightarrow \pi^*$ excitation decreases in intensity, and the $\pi \rightarrow \pi^*$ excitation involving the LUMO+1 increasingly interacts with the $n \rightarrow \pi^*$ excitations.

In summary, as χ decreases from 90 to 0°, the wavelength of maximum absorption predicted for the unprotonated aldimine changes from 389 to 423 nm. Thus a shift of as much as 30 nm can be ascribed to coplanarity of the aldimine and the PLP ring. It is also of interest to note that the predicted TDM angle ω varies with the torsion angle χ and thus with the predicted absorption wavelength. As χ decreases from 90° to 0°, ω decreases from 49° to 36°.

Conclusions

The modified INDO/S method has been shown to be capable of reliably reproducing experimental spectra for the three forms of mAspAT which have been treated in the present work. The predicted wavelengths, intensities, and polarizations of the high-

(32) Delbaere, L. T. J.; Kallen, J.; Markovic-Housley, Z.; Khomutov, A. R.; Khomutov, R. M.; Karpeisky, M. Y.; Jansonius, J. N. *Biochimie* **1989**, *71*, 449–459.

(33) Markovic-Housley, Z.; Schirmer, T.; Hohenester, E.; Clark, P. A.; Khomutov, A.; Khomutov, R. M.; Karpeisky, M. Y.; Sandmeier, E.; Christen, P.; Jansonius, J. N. *Eur. J. Biochem.*, to be submitted.

and low-pH forms of PLP are in excellent agreement with experiment, but the agreement is less satisfactory for PMP. The results reported above predict that for HPH and PMP the absorption spectrum has one major band assigned to the $\pi \rightarrow \pi^*$ excitation, as has long been the accepted interpretation.[6,18,31] However, for LPH the predicted absorption spectrum consists of two intense and two weak transitions which are close enough in energy to form a single absorption band, in agreement with the enzyme solution spectrum.

This method has also afforded an evaluation of the effects of H-bonding interactions on the spectrum of the PLP chromophore by explicitly including selected side chains of active site residues in the calculations. All H-bonding interactions considered here have led to a blue shift in the spectrum, with the single exception of the Asp222 group in LPH. In addition the effects of π-stacking interactions of Trp140 with the PLP or PMP pyridine ring were also found to lead to a blue shift.

The first aim of these studies (see Introduction), i.e., the applicability of the theoretical methods to predict the chromophore's spectrum and account for the effects due to interacting groups of mAspAT, has been satisfactorily met. Some questions remain, in particular regarding the state of protonation which may actually exist under experimental conditions. While these questions cannot be answered solely on the basis of the calculations reported here, the results discussed above lend insight into the effects of the different possible states of protonation on the spectra. The second purpose of this project, i.e., to test the sensitivity of the predicted spectrum to structural changes, has been only partly achieved by the calculations reported here. Studies in progress on the complex of mAspAT with 2-methylaspartate will provide a more rigorous test of this sensitivity.

In assessing the reliability of the calculations it has to be kept in mind that the structural data used here represent a time average of the positions available to the protein atoms in the crystal. The observed spectrum corresponds to a Boltzmann distribution of transitions obtained from distinct structures which sample the accessible points on the energy hypersurface. Thus to obtain a correct prediction of a transition energy, it would be necessary to carry out calculations for all possible geometries and then average over the Boltzmann distribution. Such an approach has been implemented for small molecules embedded in a solvent[34] but, given current computational capabilities, would be extremely expensive for systems of the size and complexity treated in this work. It is therefore gratifying that the predicted spectra agree as well as they do with the experimental ones.

Acknowledgments. The authors thank Ursula Sauder for providing the solution spectra, Margrit Jaeggi for help in preparing the diagrams, and the staff of the University of Basel's Computing Center for assistance in running the programs and for technical support. The authors gratefully acknowledge support by Swiss National Science Foundation Grants 31-26261.89 (E.L.M.) and 31-25713.88 (J.N.J.).

(34) Blair, T. J.; Krogh-Jesperson, K.; Levy, R. M. *J. Am. Chem. Soc.* **1989**, *111*, 6948-6956.

Conformational Equilibria in Amino Steroids. 2. Energetics of the Chair-Twist-Boat Equilibrium in Ring A of 3α-Hydroxy-2β-(4-morpholinyl)-5α(H)-androstan-17-one

Lee Fielding*,† and Guy H. Grant‡

Contribution from AKZO Pharma Division, Organon Laboratories Ltd., Newhouse, Lanarkshire, Scotland ML1 5SH, and The Physical Chemistry Laboratory and Oxford Centre for Molecular Sciences, University of Oxford, South Parks Road, Oxford OX1 3QZ, England.
Received August 5, 1992

Abstract: The equilibrium between chair and twist-boat conformations in ring A of the title compound has been studied by variable solvent, high-field ^{1}H and ^{13}C NMR. The distribution between chair and twist-boat forms was estimated from a consideration of vicinal ^{1}H coupling constants within the A ring and also the ^{13}C chemical shift of a "marker group" (10-methyl) that was shown to be sensitive to the conformational change. A unique aspect of the study is that the population analysis was performed in such a way that the results are not dependent on a Karplus equation. The driving force for the transition from a chair conformation to a twist-boat was found to be a fine balance between steric effects, electronic effects, and hydrogen bonding. The energy difference between the chair and twist-boat forms is near zero and ranges from -1.1 to $+1.2$ kcal mol^{-1}, depending on the medium. The intramolecular hydrogen bond contributes approximately 1.5 kcal mol^{-1} to the stability of the twist-boat conformation.

Introduction

An understanding of the preferred stereochemistry of flexible molecules is an essential prerequisite to studies of structure-activity relationships. But, just as there is no guarantee that a molecule has the same structure in solution as was found in a crystal, one cannot always safely assume that a molecule bound to a receptor has the same structure as in solution. Hence there is general interest in determining the structures and distribution between conformers of flexible molecules, particularly when the molecule is a useful drug. Steroids form the building blocks of many important and useful drugs, and it should be recognized that even steroids have flexible regions that are potentially capable of adapting in response to their environment.

We have previously shown that ring A of 3α-hydroxy-2β-(4-morpholinyl)-5α(H)-androstan-17-one (I) is flexible and adopts a chair conformation in DMSO-d_6 solution and a twist-boat conformation in $CDCl_3$.[1] In this article we explore more fully the effect of solvent on the chair-twist-boat equilibrium and show that, in the 16 solvents studied, solutions of I exist as mixtures of chair and twist-boat conformers in a dynamic equilibrium.

† Organon Laboratories Ltd.
‡ University of Oxford. Present address: Department of Biochemistry, University College, Belfield, Dublin 4, Eire.

(1) Fielding, L.; Grant, G. H. *J. Am. Chem. Soc.* **1991**, *113*, 9785-9790.

0002-7863/93/1515-1902$04.00/0